

Multi-Organ Cancer Classification and Survival Analysis

Stefan Bauer, Nicolas Carion, Joachim M. Buhmann

{BAUERS, NCARION, JBUHMANN}@INF.ETHZ.CH

Department of Computer Science

ETH Zurich

Switzerland

Peter Schüffler, Thomas Fuchs

{SCHUEFFP, FUCHST}@MSKCC.ORG

Memorial Sloan Kettering Cancer Center

New York, USA

Peter Wild

PETER.WILD@USZ.CH

Institute of Surgical Pathology

University Hospital Zurich

Switzerland

Abstract

Accurate and robust cell nuclei classification is the cornerstone for a wider range of tasks in digital and Computational Pathology. However, most machine learning systems require extensive labeling from expert pathologists for each individual problem at hand, with no or limited abilities for knowledge transfer between datasets and organ sites. In this paper we implement and evaluate a variety of deep neural network models and model ensembles for nuclei classification in renal cell cancer (RCC) and prostate cancer (PCa). We propose a convolutional neural network system based on residual learning which significantly improves over the state-of-the-art in cell nuclei classification.

However, the main thrust of our work is to demonstrate for the first time the models ability to transfer the learned concepts from one organ type to another, with robust performance. Finally, we show that the combination of tissue types during training increases not only classification accuracy but also overall survival analysis. The best model, trained on combined data of RCC and PCa, exhibits optimal performance on PCa classification and better survival group stratification than an expert pathologist ($p = 0.006$).

All code, image data and expert labels are made publicly available to serve as benchmark for the community for future research into computational pathology.

1. Introduction

To facilitate automated cancer diagnosis and prognosis, computational pathology is providing fully automated image analysis pipelines, e.g. Fuchs et al. (2008), Fuchs and Buhmann (2011) or Schueffler et al. (2010). While these results already match or surpass the classification accuracy of expert pathologists (Bicego et al., 2011), they require extensive feature engineering and extensive expert labels for specific cancer types. The ongoing success in machine learning and computer vision demonstrates the remarkable learning abilities of deep networks for image recognition (e.g. Krizhevsky et al., 2012). Deep learning algorithms have already been successfully applied in computational pathology, e.g. for the *ICPR 2012 Contest on Mitosis Detection in Breast Cancer Histological Images* Ciresan et al. (2013) and similarly for the *MICCAI 2013 Grand Challenge* (Veta et al., 2015).

There are three different approaches for employing deep neural networks: training the neural network from scratch, pre-training on a different data set or unsupervised approaches.

Pre-training follows the idea that similar features are trained in the early layers of the network and thus parameters of a trained network serve as good initializations for the same model even for a new and different data set. In the medical literature pre-training is sometimes denoted as *transfer-learning* (Shin et al., 2016). Approaches using pre-training in other medical fields have usually an order of magnitude (or even more) pictures available (Chen et al., 2015), while previous work in computational pathology has commonly focused on image representation and unsupervised feature extraction (Cruz-Roa et al., 2013; Wang et al., 2014).

While pre-training is usually applied if one does not have enough data or time to train the neural network from scratch, recent approaches for deep networks indicate that learning directly from images becomes feasible even for small data sets through thin but deep networks (He et al., 2015). Our main motivation is to investigate the performance of networks trained from scratch with fixed parameters to see the transfer of learned concepts from one organ to the next. To the best of our knowledge, there exists only very limited information on common features of cancer cells from different organs, thus potentially requiring the tailoring of current frameworks to specific cancer scoring tasks.

In 2 we describe both datasets and provide benchmark comparisons in 3. Given the typical small data sets in computational pathology, we focus on data augmentation in 3.1 and study the learning of neural networks of different depths and ensembles when trained from scratch in 3.2 and 3.3, as well as the transfer of trained networks from one organ to the next (with fixed parameters) in 3.4 and on the joint data set with two, three or four classes in 3.5. We additionally validate our results by showing that not only the classification accuracy is improved but also overall survival analysis in 4. Our approaches significantly improve over state-of-the-art in cell nuclei classification and suggest common patterns in renal cell carcinoma (RCC) and prostate cancer (PCa). In addition we provide our code and data for bench-marking and future research in computational pathology.

2. Data

Renal Cell Carcinoma (RCC) belongs to the 10 most common cancers in western societies mortality (Grignon and Che, 2005). Clear cell renal cell carcinoma (ccRCC) is a common subtype of RCC occurring on cells with clear cytoplasm. Since this cancer develops metastases in a very early stage (commonly before diagnosis), the prognosis for RCC patients is usually pessimistic Tannapfel et al. (1996). Tissue microarrays (TMA) serve as an important tool for molecular biomarker discovery, since they enable the screening of dozens or even hundreds of specimen simultaneously. Our data basis are eight ccRCC TMA images. Each image is fully labeled by two pathologists, indicating location and class of all malignant and benign cell nuclei. From 1633 found nuclei, the two pathologists agreed with the labels on 1272. These 1272 well-labeled nuclei (890 benign and 382 malignant) were extracted as patches of size 78x78 pixels centered at labeled nuclei and serve as our original study data (see Fig 1). This dataset was first published and analysed in Fuchs et al. (2008) and serves jointly with Schueffler et al. (2010) as a comparison.

Prostate cancer (PCa) is one of the most common cancer types in western male society. It is the second most frequently diagnosed cancer for human males worldwide, and the sixth leading cause of cancer related death (Jemal et al., 2011). However, research is ongoing for the development of specific biomarkers for the early diagnosis and the deeper understanding of PCa (Gillesen et al., 2010). We incorporate six new TMA images of PCa patients, twice labeled by two pathologists. From 1195 detected nuclei, they agreed on the label of 826 (207 benign, 619 malignant). Since this dataset has not been published and analysed before, we adapted and compare it with the approaches outlined in Schueffler et al. (2010) for renal cell carcinoma.

For the further analysis we only consider the subset of RCC and PCa, where the independent labels of both pathologists agree. The low inter-observer agreement of 80% illustrates the non-trivial nature of cell nucleus classification in medical imaging.

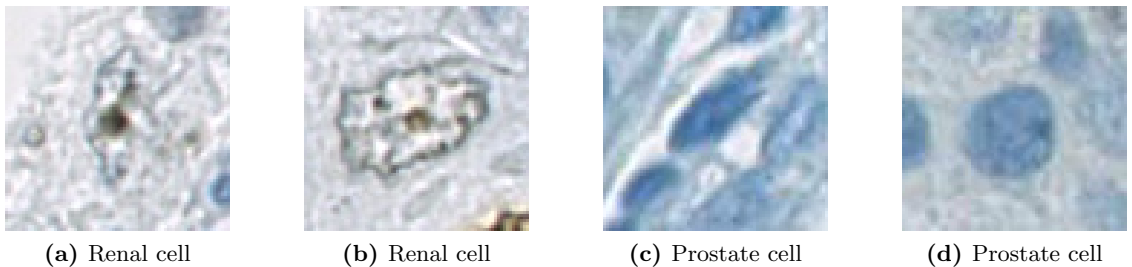


Figure 1: Examples of 78×78 patches.

3. Experiments

We used the Caffe library Jia et al. (2014) to train variants of small Cifar10 Krizhevsky and Hinton (2009), AlexNet Krizhevsky et al. (2012), ImageNet Deng et al. (2009) and googlenet Szegedy et al. (2015) like deep networks. Given our small data set we additionally implemented the newly developed residual networks He et al. (2015), which outperforms previous approaches in the ImageNet competition. A residual network with 18 layers is denoted by ResNet18 and one with 34 layers by ResNet34. All larger models e.g. ImageNet quickly led to overfitting and poor results due to the small sample size. Additionally, we tested the inclusion of custom weights in the cost function e.g. for AlexNet Krizhevsky et al. (2012), in order to overcome class biases. However, experiments showed that this compensation does not improve the error rates. While the code for the best performing ResNet's is already provided by Facebook <https://github.com/facebook/fb.resnet.torch>, we provide our code for the customized data augmentation and both data sets for bench-marking and future research. The best classifier using hand-crafted feature engineering, achieves a classification accuracy of 83% for RCC Schueffler et al. (2010), which is as good as the manual annotation: the inter-pathologist accuracy for classification of 1633 renal clear cell carcinoma nuclei is 80%. Replicating the approaches in Schueffler et al. (2010) for PCa, these values even increase up to 90%. The automated staining estimation pipeline is implemented in the free Java program TMARKER Schüffler et al. (2013). The reported performance measures are *recall*, *precision*, *F1-score* and *support*.

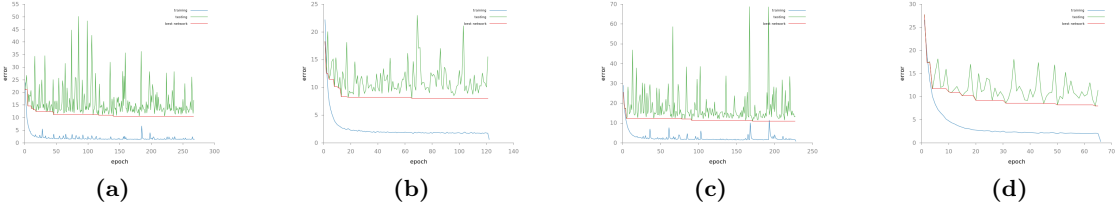


Figure 2: Examples of training (blue) and testing (green) curves of ResNet18 on (a) individual and (b) combined data of RCC and PCa. For the individual data the best net is found after 181 epochs while it is found after 65 epochs in the combined data set. The test scores fluctuate between roughly 75% and 90%, because of over-fitting, but the score of the best net steadily decreases over time (red). Examples of training and testing curves of ResNet34 on (c) individual and (d) combined data of RCC and PCa. For the individual data the best net is found after 171 epochs while it is found after 64 epochs in the combined data set.

3.1 Data augmentation

We randomly split the data into 80%, 10% and 10% for training, testing and validation. Due to the computational cost we only apply a one fold cross validation and split and average the data only once. For comparison for some nets the results of a double split experiment are reported. Given the low number of samples available one focus of our work is data augmentation and we apply the following techniques to the training set while averaging over all predictions for the validation set: firstly, the nucleus patch is *scaled down* to a randomly chosen size in [64 : 78]. After that, we select uniformly at random a *cropping* of size 64×64 , and we *mirror* it with probability 1/2. Since only the shape, and not the orientation or the color of the nuclei is discriminative for classifying it as malignant or benign Schueffler et al. (2010), we also apply a *rotation* by a random angle between 0° and 360°, and in addition *grayscaleing*. Each picture is randomly perturbed 50 times, giving altogether 60T pictures in the RCC and 40T for the PCa dataset.

3.2 RCC

Using a random partition with 80% for training and 10% for testing and validation, the performance is comparable or significantly better to the hand-crafted approach by in Schueffler et al. (2010) with a score of 83% (4b). While ResNet34 achieves only the same accuracy when the random sampling into training, testing and validation is done once, the accuracy increases with a double split and averaging to 89% (4d). Similarly the repetition of the experiment is helpful for the ResNet18 as well, even though the increase is smaller (4a and 4c). This indicates that the low performance of the ResNet34 on the single split is due to an unfavorable sampling into training and validation set and that the true performance is around 90% for both residual networks. While the overall performance of the Cifar10 net is comparable to the hand-crafted approach in Schueffler et al. (2010), it apparently has difficulties with the prediction for the malignant cells as indicated by low precision and recall (see 5a). Due to the limited number of samples in the validation set a multiple

random partitions into training, testing and validation might already reduce the chance of an unfavorable validation set, as shown for the residual networks.

Data	Precision	Recall	F1	Support
malignant	1.00	0.73	0.85	41
benign	0.89	1.00	0.94	87
Avg./Tot.	0.92	0.91	0.91	128

Data	Precision	Recall	F1	Support
malignant	0.83	0.83	0.83	41
benign	0.92	0.92	0.92	87
Avg./Tot.	0.89	0.89	0.89	128

(a) ResNet18 on RCC (double split)

(b) ResNet34 on RCC (double split)

Figure 3: Performance of networks with different layers for renal cell carcinoma.

Data	Precision	Recall	F1	Support
malignant	0.79	0.86	0.83	44
benign	0.93	0.88	0.90	84
Avg./Tot.	0.88	0.88	0.88	128

Data	Precision	Recall	F1	Support
malignant	0.79	0.68	0.73	44
benign	0.84	0.90	0.87	84
Avg./Tot.	0.83	0.83	0.82	128

(a) ResNet18 on RCC

(b) ResNet34 on RCC

Data	Precision	Recall	F1	Support
malignant	1.00	0.73	0.85	41
benign	0.89	1.00	0.94	87
Avg./Tot.	0.92	0.91	0.91	128

(c) ResNet18 on RCC (double split)

Data	Precision	Recall	F1	Support
malignant	0.83	0.83	0.83	41
benign	0.92	0.92	0.92	87
Avg./Tot.	0.89	0.89	0.89	128

(d) ResNet34 on RCC (double split)

Figure 4: Renal cell carcinoma (RCC) performance comparison of residual networks (ResNets) with different number of layers and different validation splits.

Data	Precision	Recall	F1	Support
malignant	0.72	0.75	0.73	44
benign	0.87	0.85	0.86	69
Avg./Tot.	0.81	0.81	0.81	128

(a) Cifar10 on RCC

(b) Cifar10 on PCa (full)

Figure 5: Performance of the Cifar10 trained on RCC.

3.3 PCa

In addition to the renal cell carcinoma data, we tested the different deep learning architectures on *MIB-1* stained prostate cancer TMAs. The performance for both the residual networks with 18 and 34 layers is close to the intersection of two pathologists Fig. 6a and Fig. 6b. However both nets misclassify a different patch (see Fig. 7). An ensemble of both nets with equal weights only misclassifies example (a) in Fig 7, since the confidence of the residual net with 34 layers is high enough to overcome the wrong label of the residual net with 18 layers. When trained on the combined data of RCC and PCa, all pictures (and

thus the two pictures as well) are correctly classified by both ResNet18 and ResNet34 (see Section 3.5).

Data	<i>Precision</i>	<i>Recall</i>	<i>F1</i>	<i>Support</i>
malignant	0.99	1.00	0.99	69
benign	1.00	0.93	0.96	14
Avg./Tot.	0.99	0.99	0.99	83

Data	<i>Precision</i>	<i>Recall</i>	<i>F1</i>	<i>Support</i>
malignant	0.99	1.00	0.99	69
benign	1.00	0.93	0.96	14
Avg./Tot.	0.99	0.99	0.99	83

(a) ResNet18 on PCa

(b) ResNet34 on PCa

Figure 6: Performance of networks with different layers for prostate cancer. While only one sample is misclassified for both networks, it is a different patch each time as shown in Fig. 7.

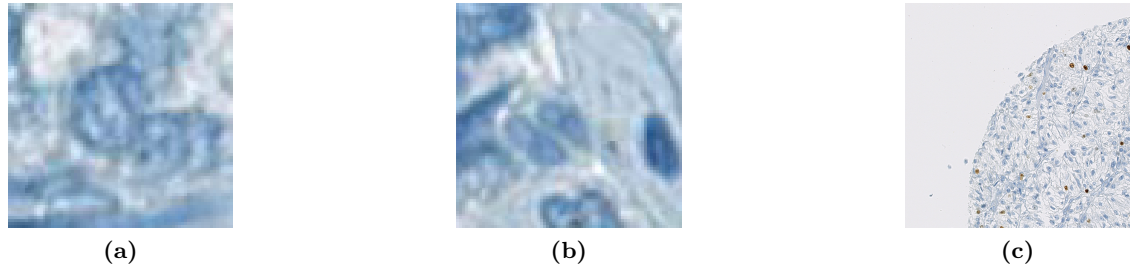


Figure 7: Misclassified examples for the 18 layer ResNet (a) and 34 layer ResNet (b) and one example image of the eight fully labeled RCC TMA image quarters.

Data	<i>Precision</i>	<i>Recall</i>	<i>F1</i>	<i>Support</i>
malignant	0.79	0.77	0.78	44
benign	0.88	0.89	0.89	84
Avg./Tot.	0.85	0.85	0.85	128

(a) Ensemble of Cifar10, ResNet18 and ResNet34 on RCC

Data	<i>Precision</i>	<i>Recall</i>	<i>F1</i>	<i>Support</i>
malignant	1.00	0.81	0.90	69
benign	0.52	1.00	0.68	14
Avg./Tot.	0.92	0.84	0.86	83

(b) Cifar10 trained on RCC and PCa and evaluated on PCa

Figure 8: Performance of an ensemble on RCC and Cifar10 trained on joint data for PCa.

3.4 Comparison of RCC trained nets on PCa and vice versa

Having trained and validated residual networks with different layers and the Cifar10 model in 3.2 and 3.3 for renal and prostate cancer, we now study the performance of the nets trained on 80% of one dataset on the full data set of the other organ. While the performance significantly drops, especially for the training on the RCC and evaluation on PCa (9a,9c, 5b), it remains significantly better on average for the training on PCa and evaluation on RCC data (9b, 9d) for both residual networks. While the average precision and recall is significantly better than random guessing in the latter case, the precision (and/or recall) for

malignant cells is close to 50%, thus indicating that only the classification of benign cells profits from learning on a different organ. The precision for malignant cells for both residual networks, being trained on RCC and evaluated on PCa even equals one. Thus agreeing with the labels of both experts. For the training on the RCC data and evaluation on the full PCa data, we even performed a double split experiment for the partition into training, testing and validation and the here reported numbers for the single split experiment fluctuated only insignificantly. When trained on RCC and evaluated on the full PCa data set, the Cifar10 net shows a similar performance as the residual networks 5b.

Data	Precision	Recall	F1	Support
malignant	1.00	0.08	0.15	619
benign	0.27	1.00	0.42	207
Avg./Tot.	0.82	0.31	0.22	826

(a) ResNet34 trained on 80% of RCC evaluated on full PCa

Data	Precision	Recall	F1	Support
malignant	0.46	0.69	0.55	382
benign	0.83	0.66	0.73	890
Avg./Tot.	0.72	0.67	0.68	1272

(b) ResNet34 trained on 80% of PCa evaluated on full RCC

Data	Precision	Recall	F1	Support
malignant	1.00	0.11	0.20	619
benign	0.27	1.00	0.43	207
Avg./Tot.	0.82	0.34	0.26	826

(c) ResNet18 trained on 80% of RCC evaluated on full PCa

Data	Precision	Recall	F1	Support
malignant	0.47	0.47	0.47	382
benign	0.77	0.77	0.77	890
Avg./Tot.	0.68	0.68	0.68	1272

(d) ResNet18 trained on 80% of PCa evaluated on full RCC

Figure 9: Performance of ResNets with different layers trained on one organ and evaluated on different one.

3.5 Multi-organ RCC and PCa data

For the multi-organ cancer classification we conducted two different kinds of experiments: first, we run a four class classification with two classes per organ (i.e. malignant and benign for prostate and malignant and benign for renal cells); second, we only used two classes (i.e. malignant and benign). The four class classification was only conducted for the residual network with 18 layers. While the evaluation on the RCC set decreases the accuracy on the validation set to 80% (see 11a), the true performance might be higher. The training accuracy is around 86% and the survival analysis in Section 4 shows a significant improvement for the RCC data. Likewise, the performance on the PCa data is improved since now no sample is miss-classified and we exactly replicate the results from the intra-pathologist agreement 11b. We regard it as a positive feature that: *No cell of one organ was labeled as cell of a different organ*. Similarly, the two-class residual networks with 18 and 34 layers trained on the combined data set have 100% accuracy on the PCa data (Fig.10b, 10d) while the performance for the RCC drops to 80%. In addition to the residual networks, the Cifar10 model trained on the joint set and validated on the PCa data achieves very good results (8b).

Data	Precision	Recall	F1	Support
malignant	0.67	0.84	0.75	44
benign	0.90	0.79	0.84	84
Avg./Tot.	0.82	0.80	0.81	128

(a) ResNet18 trained on RCC and PCa and evaluated on RCC (benign and malignant)

Data	Precision	Recall	F1	Support
malignant	0.71	0.68	0.70	44
benign	0.84	0.86	0.85	84
Avg./Tot.	0.79	0.80	0.80	128

(c) ResNet34 trained on RCC and PCa and evaluated on RCC (benign and malignant)

Data	Precision	Recall	F1	Support
malignant	1.00	1.00	1.00	69
benign	1.00	1.00	1.00	14
Avg./Tot.	1.00	1.00	1.00	83

(b) ResNet18 trained on RCC and PCa and evaluated on PCa (benign and malignant)

Data	Precision	Recall	F1	Support
malignant	1.00	1.00	1.00	69
benign	1.00	1.00	1.00	14
Avg./Tot.	1.00	1.00	1.00	83

(d) ResNet34 trained on RCC and PCa and evaluated on PCa (benign and malignant)

Figure 10: Performance for ResNet with 18 and 34 layers for a two class classification.

Data	Precision	Recall	F1	Support
malignant	0.73	0.68	0.71	44
benign	0.84	0.87	0.85	84
Avg./Tot.	0.80	0.80	0.80	128

(a) ResNet18 trained on RCC and PCa and evaluated on RCC (four classes)

Data	Precision	Recall	F1	Support
malignant	1.00	1.00	1.00	69
benign	1.00	1.00	1.00	14
Avg./Tot.	1.00	1.00	1.00	83

(b) ResNet18 trained on RCC and PCa and evaluated on PCa (four classes)

Figure 11: Performance of ResNet18 for a four class classification (i.e. two classes for each organ).

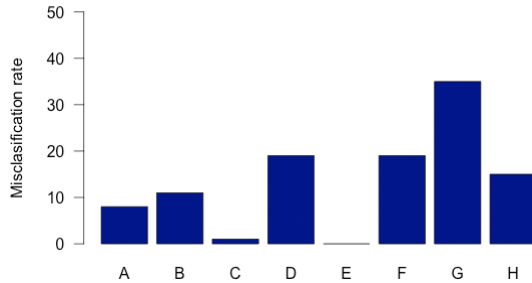


Figure 12: Averaged misclassification error for different networks. **A:** ResNet18 on RCC, double split, **B:** ResNet34 on RCC, double split, **C:** ResNet18 and ResNet34 on PCa, **D:** ResNet18 and ResNet34 trained on combined data set for two classes evaluated on RCC, **E:** ResNet18 on combined data for two classes and four classes, evaluated PCa, **F:** Cifar10 on RCC, **G:** ResNet18 on RCC evaluated on PCa, **H:** Ensemble of Cifar10, ResNet18 and ResNet34 on RCC.

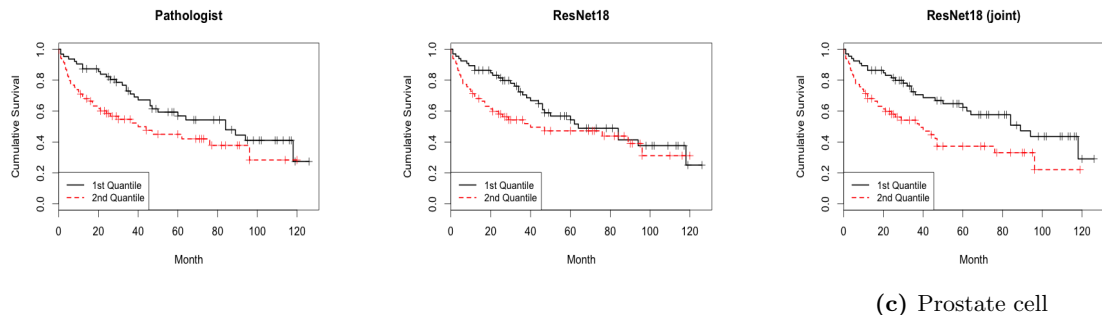
Fig 12 presents an overview of the classification error of our best models.

4. Survival Analysis

In addition to classification, we tested our approaches on follow-up survival data on 132 RCC patient. In RCC, the staining estimate of the proliferation protein *MIB-1* is corelated with the overall survival outcome. The staining estimate is the relative amount of stained cells *among the cancer cells* in the image. Therefore, a cell classification process is crucial for robust automated survival analysis.

On 132 TMA images of RCC patients 130,899 cell nuclei have been detected earlier, as well as labeled as stained or not. For accurate staining estimation, we extract the

nuclei as 78×78 px patches and classify them into malignant or benign with the proposed models and compare the staining estimate to a trained pathologist. The patients have been stratified into two equally sized groups and the Kaplan-Meier survival estimator is plotted. The log rank test was used to test for significant survival differences between the patient groups (see Fig. 16). While the benefit for training on the combined data set of both organs was not evident by the performance measures in 3.5, the residual net with 18 layers outperforms the human pathologist (Fig. 16) and previous approaches Fuchs et al. (2008) as indicated by a p-value of 0.006 for the ResNet18 compared to a p-value of 0.038 for the pathologist. While training on the combined set led to a significant gain for the residual network with 18 layers it does not help improving the model with 34 layers. This indicates that the smaller model finds a good balance between complexity and available data. The four class classification has a higher p-value for the residual network with 18 layers compared to the two class network trained on RCC alone and the combined data with two classes.



(c) Prostate cell

Figure 13: Kaplan-Meier estimators based on the manual estimates of a pathologist (**left**), the predictions of ResNet18 trained on RCC alone (**middle**), and the prediction of ResNet18 trained on the joint data set of RCC and PCa (**right**).

5. Conclusion

Histologic nuclei classification is a crucial precursor for a plethora of research tasks in computational pathology. In this paper we proposed a deep learning framework for application on *MIB-1* stained renal cell cancer and prostate cancer tissue microarrays. Our contributions are (i) developing and providing extensive data augmentation procedures (ii) the detailed evaluation of various state-of-the art convolutional neural network (CNN) architectures, (iii) the implementation of multi-organ prediction models, (iv) the evaluation of CNN ensemble models and (v) the application to survival analysis of RCC patients.

Training on the combined set of RCC and PCa improves the score up to zero misclassifications for residual networks and achieves in addition very good results with the Cifar10 net on the prostate cancer data set. For the smaller residual network with 18 layers, the training on the combined data set indicates a good trade-off between model-complexity and available data and leads to significantly improved survival curves in terms of survival difference ($p = 0.006$). Jointly with the insight that a four class classification does not

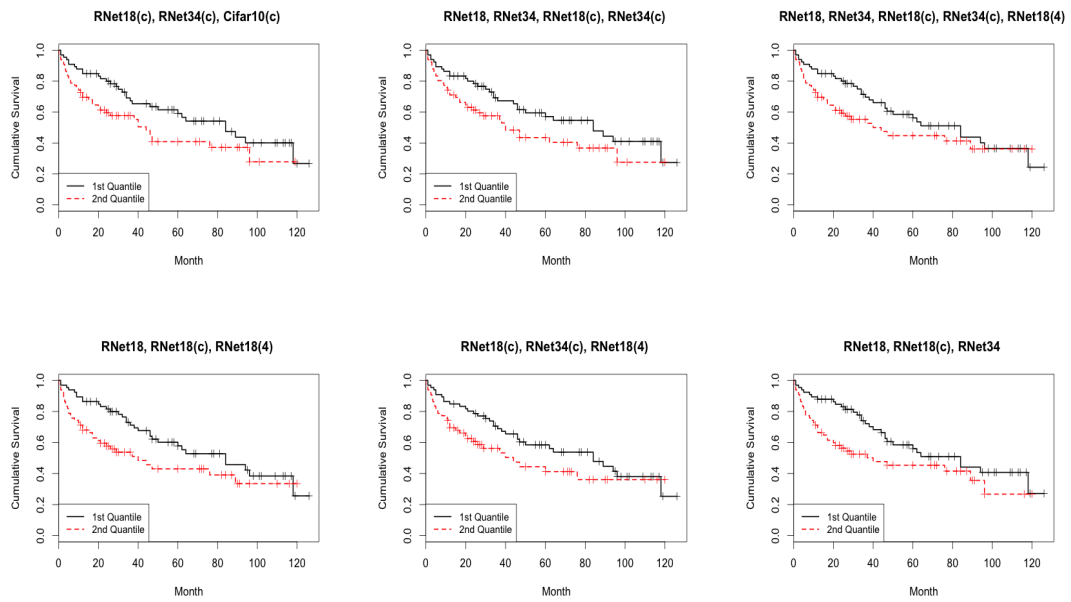


Figure 14: Kaplan Meier estimators for different ensembles of deep neural networks. For ResNet18(c) and ResNet34(c), the (c) indicates that the net was trained on the combined PCA and RCC data. RNet4 stand for a residual net with 18 layers that was trained for four classes i.e. two classes per organ.

lead to improved results compared to a two-class classification, we find evidence supporting common features for multi-organ cancer detection.

We are convinced that the proposed pipeline, together with the published code, image datasets, and survival information will serve as an useful and extensive benchmark for future computational research to the whole community.

References

Manuele Bicego, Aydn Ula, Peter J. Schüffler, Umberto Castellani, Vittorio Murino, Andr Martins, Pedro Aguiar, and Mario Figueiredo. Renal Cancer Cell Classification Using Generative Embeddings and Information Theoretic Kernels. In *Pattern Recognition in Bioinformatics*, volume 7036, pages 75–86. 2011. ISBN 978-3-642-24854-2.

Hao Chen, Dong Ni, Jing Qin, Shengli Li, Xin Yang, Tianfu Wang, and Pheng Ann Heng. Standard plane localization in fetal ultrasound via domain transferred deep neural networks. *Biomedical and Health Informatics, IEEE Journal of*, 19(5):1627–1636, 2015.

Dan Ciresan, Alessandro Giusti, Luca Gambardella, and Jürgen Schmidhuber. Mitosis detection in breast cancer histology images with deep neural networks. *Medical Image Computing and Computer-Assisted Intervention MICCAI*, 2013.

Angel Cruz-Roa, John Edison Arevalo Ovalle, Anant Madabhushi, and Fabio A. González. A deep learning architecture for image representation, visual interpretability and automated basal-cell carcinoma cancer detection. *Medical Image Computing and Computer-Assisted Intervention MICCAI*, 2013.

Jia Deng, Wei Dong, Richard Socher, Li-Jia Li, Kai Li, and Li Fei-Fei. ImageNet: A large-scale hierarchical image database. In *CVPR*, pages 248–255. IEEE, 2009. ISBN 978-1-4244-3992-8. doi: 10.1109/cvpr.2009.5206848.

Thomas J. Fuchs and Joachim M. Buhmann. Computational Pathology: Challenges and Promises for Tissue Analysis. *Computerized Medical Imaging and Graphics*, 35(78):515–530, 2011. ISSN 0895-6111. doi: 10.1016/j.compmedimag.2011.02.006.

Thomas J. Fuchs, Peter J. Wild, Holger Moch, and Joachim M. Buhmann. Computational Pathology Analysis of Tissue Microarrays Predicts Survival of Renal Clear Cell Carcinoma Patients. In *Medical Image Computing and Computer-Assisted Intervention MICCAI*, volume 5242, pages 1–8. Springer-Verlag, 2008. ISBN 978-3-540-85989-5. doi: 10.1007/978-3-540-85990-1_1.

S Gillessen, I Cima, R Schiess, P Wild, M Kalin, P Schueffler, JM Buhmann, H Moch, R Aebersold, and W Krek. Cancer genetics-guided discovery of serum biomarker signatures for prostate cancer. In *ASCO Annual Meeting Proceedings*, volume 28, page 4564, 2010.

David J Grignon and Mingxin Che. Clear cell renal cell carcinoma. *Clinics in laboratory medicine*, 25(2):305–316, 2005.

Kaiming He, Xiangyu Zhang, Shaoqing Ren, and Jian Sun. Deep residual learning for image recognition. *arXiv preprint arXiv:1512.03385*, 2015.

Ahmedin Jemal, Freddie Bray, Melissa M Center, Jacques Ferlay, Elizabeth Ward, and David Forman. Global cancer statistics. *CA: a cancer journal for clinicians*, 61(2):69–90, 2011.

Yangqing Jia, Evan Shelhamer, Jeff Donahue, Sergey Karayev, Jonathan Long, Ross Girshick, Sergio Guadarrama, and Trevor Darrell. Caffe: Convolutional architecture for fast feature embedding. *arXiv preprint arXiv:1408.5093*, 2014.

Alex Krizhevsky and Geoffrey Hinton. Learning multiple layers of features from tiny images, 2009.

Alex Krizhevsky, Ilya Sutskever, and Geoffrey E. Hinton. Imagenet classification with deep convolutional neural networks. In *Advances in Neural Information Processing Systems 25*, pages 1106–1114. 2012.

Peter J. Schueffler, Thomas J. Fuchs, Cheng Soon Ong, Volker Roth, and Joachim M. Buhmann. Computational TMA Analysis and Cell Nucleus Classification of Renal Cell Carcinoma. In *Proc. of 32nd DAGM conference on Pattern recognition*, pages 202–211, 2010. ISBN 3-642-15985-0 978-3-642-15985-5.

Peter J. Schüffler, Thomas J. Fuchs, Cheng S. Ong, Peter Wild, and Joachim M. Buhmann. TMARKER: A Free Software Toolkit for Histopathological Cell Counting and Staining Estimation. *Journal of Pathology Informatics*, 4(2):2, 2013.

Hoo-Chang Shin, Holger R Roth, Mingchen Gao, Le Lu, Ziyue Xu, Isabella Nogues, Jianhua Yao, Daniel Mollura, and Ronald M Summers. Deep convolutional neural networks for computer-aided detection: Cnn architectures, dataset characteristics and transfer learning. 2016.

Christian Szegedy, Wei Liu, Yangqing Jia, Pierre Sermanet, Scott Reed, Dragomir Anguelov, Dumitru Erhan, Vincent Vanhoucke, and Andrew Rabinovich. Going deeper with convolutions. In *CVPR*, 2015.

Andrea Tannapfel, Helmut A Hahn, Alexander Katalinic, Rainer J Fietkau, Reinhard Kuehn, and Christian W Wittekind. Prognostic value of ploidy and proliferation markers in renal cell carcinoma. *Cancer*, 77(1):164–171, 1996.

Mitko Veta, Paul J Van Diest, Stefan M Willems, Haibo Wang, Anant Madabhushi, Angel Cruz-Roa, Fabio Gonzalez, Anders BL Larsen, Jacob S Vestergaard, Anders B Dahl, et al. Assessment of algorithms for mitosis detection in breast cancer histopathology images. *Medical image analysis*, 20(1):237–248, 2015.

Haibo Wang, Angel Cruz-Roa, Ajay Basavanhally, Hannah Gilmore, Natalie Shih, Mike Feldman, John Tomaszewski, Fabio A. González, and Anant Madabhushi. Cascaded ensemble of convolutional neural networks and handcrafted features for mitosis detection. *International Society for Optics and Photonics SPIE Medical Imaging*, 2014.

Appendix A.

Data	Precision	Recall	F1	Support
malignant	0.97	0.11	0.20	619
benign	0.27	0.99	0.43	207
Avg./Tot.	0.80	0.33	0.25	826

(a) ResNet18 trained on RCC and evaluated on PCa (double split)

Data	Precision	Recall	F1	Support
malignant	1.00	0.08	0.15	619
benign	0.27	1.00	0.42	207
Avg./Tot.	0.82	0.31	0.22	826

(b) ResNet34 trained on RCC and evaluated on PCa (double split)

Figure 15: Impact of a double split and averaging for the random sampling for the partition into 80%, 10% and 10% of data for training, validation and cross-validation.

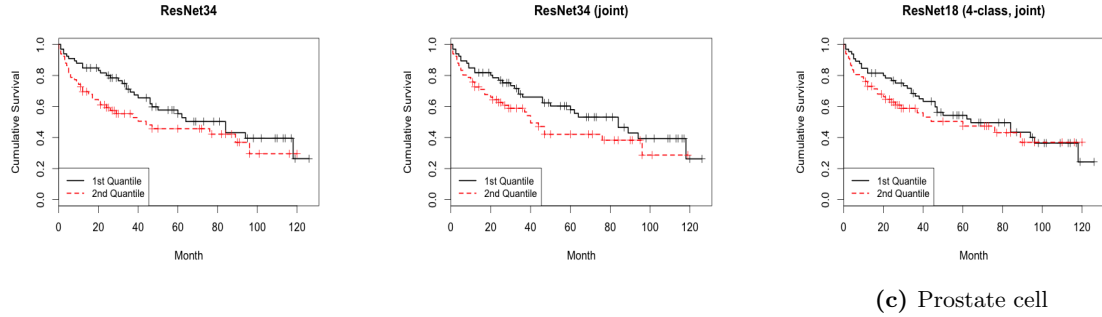


Figure 16: Kaplan Meier estimators for the ResNet34 trained on RCC alone and on the joint data set of RCC and PCa and for the four class ResNet18 trained on the combined data set.